

# Parametric Investigation on Dynamics of Toner and Carrier Particles in Electrophotographic Two-Component Magnetic Brush Development System Using Direct Observation Technique and Numerical Simulation

Hiroyuki Kawamoto; Dept. of Applied Mechanics and Aerospace Engineering, Waseda University; 3-4-1, Okubo, Shinjuku, Tokyo 169-8555, Japan; kawa@waseda.jp

## Abstract

The author has studied the dynamics of toner and carrier particles in a two-component magnetic brush development system used for electrophotography using a direct observation technique and numerical simulation method. We have manufactured a mock-up apparatus consisting of a pseudo-photoreceptor drum, development sleeve, and stationary magnetic roller. The image was created on an insulated film electrode pasted onto the drum. The behavior of the toner and carrier particles has been observed directly using a high-speed microscope camera and calculated using 3D distinct element method that includes the calculation of the magnetic interaction force and the transient electric conduction in carrier chains. Parameters for the experiment and calculation were the diameters of toner and carrier particles, toner/carrier concentration, development gap, development voltage, speed ratio between the photoreceptor drum and development sleeve, waveform and magnitude of superposed ac development voltage, and distribution of magnetic field created by the magnetic roller. Optimum conditions for realizing high image quality printing have been proposed considering all the various factors together.

## Introduction

Statics and dynamics of toner and carrier particles are of great interest in a two-component magnetic brush development system adopted in color and/or high-speed electrophotography machines [1-17]. As shown in Fig. 1, magnetic carrier beads with electrostatically attached toner particles are introduced into the vicinity of a rotatory sleeve with a stationary magnetic roller inside it. Diameter of carrier particle is several tens micrometer and that of the toner particle is about 6  $\mu\text{m}$ . Magnetized carrier beads form chain clusters on the sleeve in the magnetic field. Tips of chains touch the photoreceptor surface at the development area and toner particles on chains move to electrostatic latent images created by a laser beam on the photoreceptor to form real images [1-3].

Although the system can achieve relatively high quality of printing in comparison with other systems, such as the nonmagnetic single-component system, they occasionally produce certain image defects such as a pale defect of halftone following solid image [4] and bead-carry-out [1,5-7]. Many experimental and numerical investigations have been conducted in order to clarify the mechanisms of these defects and to propose effective countermeasures against them. However, the effect of system parameters has not been thoroughly clarified, and therefore its design and improvement rely heavily on trial and error.

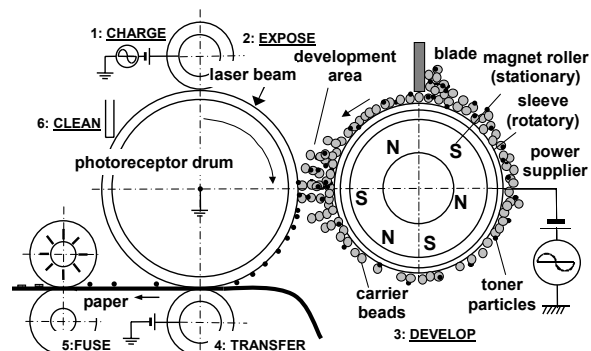


Figure 1. Schematic drawing of two-component magnetic brush development system in electrophotography.

In this study, a numerical and experimental investigation was carried out on the development process to clarify the effects of parameters such as the diameters of toner and carrier particles, toner/carrier concentration, development gap, development voltage, speed ratio between the photoreceptor drum and development sleeve, waveform and magnitude of superposed ac development voltage, and distribution of magnetic field created by the magnetic roller. The numerical calculation is based on the combination of finite differential calculation of electromagnetic field and 3D calculation of particle motion using the discrete element method [3,8,11-17]. The calculated results were weighed with the measurement of developed toner profile and direct observation of particle motion in the development area using high-speed microscope camera [6-9]. Optimum conditions for realizing high image quality printing have been proposed considering all the various factors together.

## Experimental

A model machine, as shown in Fig. 2, was used in the experiment instead of a commercial printer [4,7]. This machine consisted of a short photoreceptor drum, a development sleeve, a magnetic roller, and the driving systems. The drum and development sleeve were 30 and 18 mm in diameter, respectively. The rotational speed of the drum was 150 mm/s, and that of the development sleeve can be altered. The magnetic flux density at the surface of the sleeve was 120 mT normal to the gap at the center of the development area. The drum, which was made of aluminum, was not coated with a photoreceptor; however, it was coated with a nonconductive tape (thickness: 90  $\mu\text{m}$ ) because high-intensity light had to be used in

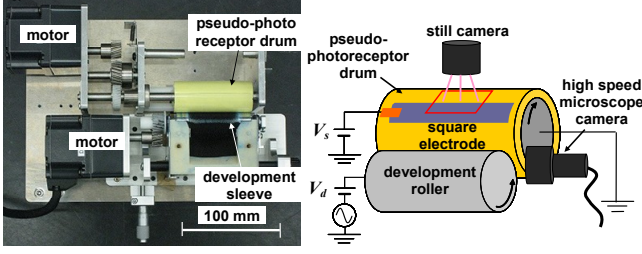


Figure 2. Apparatus used to model a two-component magnetic brush development system.

order to observe the motion of the carrier and toner particles in the development area with a high-speed microscope camera. An electrostatic solid latent image was formed by using an electrode that was made of aluminum foil (width: 0.5 mm, thickness: 10  $\mu\text{m}$ ) and insulated with polyimide tape (thickness: 75  $\mu\text{m}$ ). Upon application of a dc voltage to the electrode, the electrode generated an electrostatic latent image that was similar to a latent image created on an actual photo-receptor drum. An ac voltage was superposed onto the dc voltage.

Spherical soft magnetic carrier particles and pulverized non-magnetic toner particles were used in the experiment. The magnetic carrier particles were composed of soft ferrite, and the toner particles were cyan pigmented with an average diameter of 6  $\mu\text{m}$ .

## Numerical Calculation

A numerical simulation tool based on the distinct element method has been developed. The following motion equations are solved for each particle.

$$m_j \ddot{\mathbf{u}}_j = \mathbf{F}_j, \quad I_j \ddot{\boldsymbol{\varphi}}_j = \mathbf{M}_j, \quad (1)$$

where  $m_j$ ,  $\mathbf{u}_j$  ( $= x_j, y_j, z_j$ ),  $I_j$ ,  $\boldsymbol{\varphi}_j$  ( $= \varphi_{xj}, \varphi_{yj}, \varphi_{zj}$ ),  $\mathbf{F}_j$ , and  $\mathbf{M}_j$  are mass, displacement vector, moment of inertia, rotation angle, applied force vector, and moment applied to a particle  $j$ , respectively. In this study, mechanical interaction force, magnetic force, electrostatic force, van del Waals force, air drag, and gravitational force are included in the applied force and momentum.

The mechanical interaction force in the normal and tangential directions is estimated based on Voigt model from Hertzian contact theory and Mindlin contact theory, respectively [8].

The magnetic force  $\mathbf{F}_{mj}$  and rotational moment  $\mathbf{M}_{mj}$  of the  $j$ -th particle with the magnetic moment  $\mathbf{p}_j$  are given by the following expressions, under the assumption that each particle behaves as a magnetic dipole placed at the center of the magnetized particle [3, 8, 11-17].

$$\mathbf{F}_{mj} = (\mathbf{p}_j \cdot \nabla) \mathbf{B}_j, \quad \mathbf{M}_{mj} = \mathbf{p}_j \times \mathbf{B}_j. \quad (2)$$

The magnetic dipole moment  $\mathbf{p}_j$  and magnetic flux density  $\mathbf{B}_j$  at the position of the  $j$ -th particle are

$$\mathbf{B}_j = \mathbf{B}_j^1 + \sum_{\substack{k=1 \\ j \neq k}}^N \mathbf{B}_{kj}, \quad \mathbf{p}_j = \frac{4\pi}{\mu_0} \frac{\mu - 1}{\mu + 2} r_j^3 \mathbf{B}_j, \quad \mathbf{B}_{kj} = \frac{\mu_0}{4\pi} \left( \frac{3\mathbf{p}_k \cdot \mathbf{r}_{kj}}{r_{kj}^5} \mathbf{r}_{kj} - \frac{\mathbf{p}_k}{r_{kj}^3} \right), \quad (3)$$

where  $N$  is the number of particles;  $\mu_0$ , the magnetic permeability of free space, and  $\mu$ , the relative permeability of the particles.  $\mathbf{B}_j^1$ , the applied magnetic field generated by the magnetic roller,  $\sum \mathbf{B}_{kj}$ , the field at the  $j$ -th particle due to the dipoles of the remaining  $N-1$

particles, and  $\mathbf{r}_{kj}$ , the position vector from the  $k$ -th to the  $j$ -th particle.

The Coulomb force  $\mathbf{F}_e$  applied to a charged carrier or toner particle is calculated by integrating  $\rho \mathbf{E}$  over the volume  $V$  of the particle. The charge density  $\rho$  of the particle and the electrostatic field  $\mathbf{E}$  are calculated by solving the following coupled partial differential equations [3,9].

$$\nabla \cdot (\varepsilon \mathbf{E}) = \rho, \quad -\frac{\partial \rho}{\partial t} = \nabla \cdot (\sigma \mathbf{E}), \quad (4)$$

where  $\varepsilon$  and  $\sigma$  are the permittivity and the conductivity of the particle, respectively. Equation (4) indicates that the model can evaluate the effects of the conductivity of carrier particles as well as the transient charge distribution in the carrier particles. Here, the iterative finite differential method is used for numerical calculation of the charge density  $\rho$  and the electrostatic field  $\mathbf{E}$ .

Van del Waals force  $\mathbf{F}_v$ , air drag  $\mathbf{F}_a$ , and gravitational force  $\mathbf{F}_g$  are calculated by the following equations.

$$\mathbf{F}_v = -\frac{AX}{12h^2} \left( X = \frac{d_1 d_2}{d_1 + d_2} \right), \quad \mathbf{F}_{aj} = -6\pi\eta r_j \dot{\mathbf{u}}_j, \quad \mathbf{F}_{gj} = m_j \mathbf{g}, \quad (5)$$

where  $d$  is the diameter of particle,  $X$  is Hamaker constant,  $h$  is the distance between particles,  $\eta$  is the viscosity of air and  $\mathbf{g}$  is the gravitational acceleration.

An excessive amount of time is required for numerical calculation with the above method. The calculation time is critically dependent on the process of detecting contact between small toner and relatively large carrier particles, the calculation of the magnetic interaction force between magnetized carrier particles, and the calculation of the electrostatic force at each time step. In this regard, the computation time is reduced by detecting contact within virtual cells that include all adjacent particles. Other measures include the simplification of the geometry, the adoption of periodical boundary conditions that enable the chain formation to be a realistic manner, the calculation of magnetic interaction force within restricted area, and the omission of magnetic and electrostatic force calculations for several time steps. In addition to these improvements on the numerical algorithm, parallel computing was conducted with OpenMP and CUDA.

## Results and Discussion

### Chain Formation

Chain formation and development process was examined. Figure 3 shows calculated and observed behavior of chains at the development gap [8]. The calculated result agreed fairly well to the observed, and the calculation deduces dynamic and differential characteristics of the process that can not be clarified by the experiment. At the inlet of the development area, the magnetic carrier particle chains became parallel to the magnetic field, come in con-

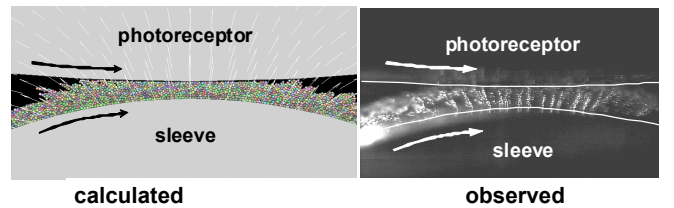


Figure 3. Calculated and observed behavior of chains at development gap.

tact with the photoreceptor drum, and are depressed by the drum. The brush is depressed to backward before the chains reach the center of the development gap when the sleeve speed exceeds the drum speed, and spring just before the chains become free. The spring-back of the chains to their normal states behind the development area appears to cause a stripe defect of the toner images developed on the photoreceptor if the force exerted by the brush on the photoreceptor is very high. The slip speed is independent of the diameter of the carrier particles. The friction force exerted by the brush on the photoreceptor drum increases in accordance with the increase in the magnetic flux density and decreases with an increase in the brush length; however, the diameter of the particles does not affect the total force. Although the total force exerted on the photoreceptor is almost independent of the diameter of the carrier particles, the differential force exerted by individual chains is small and distributes dense in the case of small particles; on the other hand, it is large and distributes rough in the case of large particles. Small carrier particles are advantageous in preventing any disturbances in the images developed on the photoreceptor. The friction force and the density of chains that come in contact with the photoreceptor drum are large when the doctoring gap is large or the development gap is small. When these parameters exceed the threshold, the pressure and the density increase drastically. The gap between the doctor blade and the photoreceptor drum must be determined so that the amount of carrier particles supplied to the development area is moderate.

### Development Characteristics

The numerical calculation (Fig. 4) and direct observation show that adhesion of toner particles to a latent image on the photoreceptor occurred not only in the contact area between the carrier brush and the photoreceptor but also in the pre- and postnip regions where the carrier brush did not come into contact with the photoreceptor [7]. At the prenip region, carrier chains vibrated in the lateral direction when the leaning chains became erect due to the abrupt change of the magnetic flux line, and, at the same time, toner particles were forced to separate from the inside of the chain. The separated airborne toner particles adhered to the latent image. At the postnip region, toner particles separated from the chain and formed a toner cloud in the gap. The toner cloud vibration synchronized with the frequency of the ac voltage, and some portion of the airborne toner adhered to the latent image. The toner particles were developed above the threshold voltage, and the number of developed toner particles increased with the dc development voltage, toner concentration, and speed ratio. Measured and calculated relationships between the applied electric field and the averaged toner height are shown in Fig. 5.

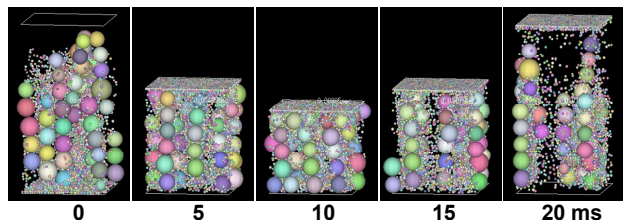


Figure 4. An example of calculated motions of toner and carrier particles in development gap (upper: photoreceptor drum, lower: development sleeve).

### Pale Defect of Halftone Following Solid Image

A pale image defect observed in the halftone area following a solid image was investigated [4]. It was clarified that the pale image defect was caused by the movement of toner particles from the halftone area to the edge of the solid image on the photoreceptor drum in the pre-nip region. The circumferential electrostatic field between the halftone area and solid area on the photoreceptor drum was the driving force of the toner motion. The local concentration of airborne toner particles at the edge of the solid image was another cause of the pale image defect. Preferred methods for reducing the pale image defect include the application of high ac voltage and the adoption of a high sleeve speed to drum speed ratio and small development gap.

### Bead-Carry-Out (BCO)

The BCO phenomenon [6,7] was apt to take place at the condition of the positive voltage application than that of the negative voltage application. Toner particles were developed on the drum when the negative voltage was applied. The reason for the occurrence of this phenomenon is simple: because the photoreceptor was covered with negatively charged toner particles when the toner particles were adhered to the photoreceptor, the effective voltage at the development gap was reduced by the surface voltage. The reduction in the surface voltage due to the application of the dc voltage was confirmed experimentally [7]. It can be clearly observed that the surface voltage was induced when the dc voltage was applied. The induction in the surface voltage was almost independent of the toner concentration, but it decreased slightly when the toner concentration was low. In any case, the induced voltage was lower than the applied dc development voltage, especially when the speed ratio and toner concentration were low, probably because a reduction in the concentration of toner particles in the brush in the image area caused an increase in the counter charge of the brush. The second observation was that the number density of the adhered carrier particles was high when the toner concentration was low. Because insulative toner particles disturbed the electrical conduction of the brush, the electrical charge at the top of the chains, which was induced by the applied voltage, decreased above the critical concentration of toner particles in the brush. This decrease in the electrical charge caused a reduction in the Coulomb force applied to the top of the chains, and the BCO phenomenon was improved when a sufficient concentration of toner particles was added to the carrier brush [5]. The number density of the adhered carrier particles was also high when the speed ratio of the develop-

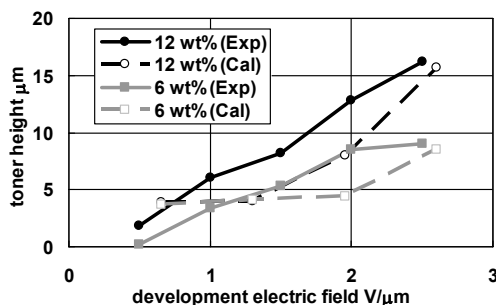


Figure 5. Relationship between development electric field and averaged height of developed toner piles.

ment sleeve to photoreceptor drum was low. There could be two possible reasons why the BCO phenomenon occurred when the speed ratio was low. One was the shortage of toner particles in the brush, as was the case when the initial toner concentration was low. When the rotational speed of the development sleeve was low, a concentration of toner particles was diluted in the brush at the post-nip region and a relatively large Coulomb force was applied to the top of the chains. The other possible reason could be that the surface voltage of the latent image was not sufficiently neutralized at the low speed ratio due to a shortage of developed toner particles on the photoreceptor drum. This hypothesis was supported by the experimental result; the surface voltage approached the applied dc voltage when the speed ratio was high, but it deviated from the applied dc voltage when the speed ratio was low.

## Conclusion

Parametric investigation on the dynamics of toner and carrier particles in electrophotographic two-component magnetic brush development system has been investigated by carrying out the measurement of developed toner profiles, direct observations with a high-speed microscope camera, and numerical calculations based on the improved distinct element method. The calculated results agreed reasonably well with the experimental observations. The experimental and numerical results are used for the improvement of the two-component development system in electrophotography.

The author wishes to thank K. Hiratsuka, S. Iesaka, T. Muroga and S. Watanabe (Waseda University) for their help in carrying out the research. This research was supported by the Samsung Yokohama Research Institute (SYRI). SYRI provided the mock-up machine, carrier, and toner particles.

## References

- [1] E. M. Williams, *The Physics and Technology of Xerographic Processes* (Krieger, Huntington, NX, 1993).
- [2] L. B. Schein, *Electrophotography and Development Physics*, 2nd ed. (Laplacian Press, Morgan Hill, CA, 1996).
- [3] K. Hirakura and H. Kawamoto, *Electrophotography -Process and Simulation* (Tokyo Denki University Press, Tokyo, 2008).
- [4] H. Kawamoto, S. Iesaka, T. Muroga and S. Watanabe, Pale Defect of Halftone Following Solid Image in Two-Component Magnetic Brush Development System in Electrophotography, *IS&T's NIP27*, Minneapolis (2011) pp.113-116.
- [5] N. Nakayama, Y. Watanabe, Y. Watanabe and H. Kawamoto, Experimental and Numerical Study on the Bead-Carry-Out in Two-Component Development Process in Electrophotography, *J. Imaging Sci. Technol.*, 49, 5 (2005) pp.539-544.
- [6] H. Kawamoto, Bead-Carry-Out Phenomenon in Two-Component Development System of Electrophotography, *IS&T's NIP24*, Pittsburgh (2008) pp.309-312.
- [7] H. Kawamoto and S. Iesaka, Characteristics of Development and Bead-Carry-Out Phenomena in Two-Component Electrophotographic Development System, *J. Imaging Sci. Technol.*, 55, 3, (2011), pp.030507-1-6.
- [8] H. Kawamoto and T. Hiratsuka, Statics and Dynamics of Carrier Particles in Two-Component Magnetic Development System in Electrophotography, *J. Imaging Sci. Technol.*, 53 (2009) pp.060201-1-10.
- [9] H. Kawamoto, Direct Observation and Numerical Study on Dynamics of Toner Particles in Magnetic Single-Component Development System of Electrophotography, *IS&T's NIP24*, Pittsburgh (2008) pp.325-328.
- [10] H. Yamamoto, Y. Takashima, T. Matsumura, M. Kuroda and Y. Hayashi, Developer with Magnetic Resinous Toner and Micro-Carrier, *J. Imaging Sci. Technol.*, 35, 2 (1991) pp.119-124.
- [11] T. Kubota, H. Inoue, Y. Iino and J. Hidaka, Numerical Analysis for Behavior of Developer in Magnetic Brush System by the Particles Method, *IS&T's NIP 16*, Vancouver (2000) pp.751-755.
- [12] N. Nakayama, H. Kawamoto and M. Yamaguchi, Statics of Magnetic Bead Chain in Magnetic Field, *J. Imaging Sci. Technol.*, 46, 5 (2002) pp.422-428.
- [13] T. Watanabe, Numerical Simulation of Carrier Behavior around a Magnet Roller in Two-Component Developer Unit in Electrophotography, *IS&T's NIP 21*, Baltimore (2005) pp.578-581.
- [14] H. Mio, A. Shimosaka, Y. Shirakawa and J. Hidaka, Cell Optimization for fast contact detection in the discrete element method algorithm, *Advanced Powder Technology*, 18, 4 (2007) pp.441-453.
- [15] M. Nakano, The Study of the Difference of Toner-Motion Among Several Development Systems, *IS&T's NIP24*, Pittsburg (2008) pp.299-302.
- [16] N. Nakayama, T. Ito, Y. Watanabe, N. Hirooka and T. Seko, Simulation of Two-Component Development Process for Frontloading Design, *IS&T's NIP25*, Louisville (2009) pp.241-244.
- [17] H. Mio, J. Kawamura, R. Higuchi, A. Shimosaka, Y. Shirakawa and J. Hidaka, Effect of Toner Charge on Developing Behavior in Two-Component Electrophotographic System by Discrete Element Method, *J. Imaging Sci. Technol.*, 53, 1 (2009), pp.010505-1-8.
- [18] R. S. Paranjpe and H. G. Elrod, Stability of chains of permeable spherical beads in an applied magnetic field, *J. Appl. Phys.*, 60, 1 (1986) pp.418- 422.

## Author Biography

*KAWAMOTO, Hiroyuki holds a BS degree from Hiroshima Univ. (1972) and a Dr. degree from Tokyo Institute of Technology (1983). From 1972 to 1991 he was a Senior Engineer at Hitachi Ltd. In 1991 he moved to Fuji Xerox, and had been engaged in the research of electrophotography. In 1999 he left Fuji Xerox and he is now a professor of Waseda Univ. in Tokyo. He was selected a Fellow of the IS&T in 1999 and awarded Carlson Award in 2007 and Journal Award in 2010.*